Mon. Not. R. Astron. Soc. **290,** 577–584 (1997)

The extended radio emission in the luminous X-ray cluster A3667

H. J. A. Röttgering,[1,2,3] M. H. Wieringa,[4] R. W. Hunstead[5] and R. D. Ekers[6]

[1]*Leiden Observatory, PO Box 9513, 2300 RA, Leiden, The Netherlands*
[2]*Mullard Radio Astronomy Observatory, Cavendish Laboratory, Madingley Road, Cambridge CB3 0HE*
[3]*Institute of Astronomy, Madingley Road, Cambridge CB3 0HA*
[4]*ATNF, Locked Bag 194, Narrabri NSW 2390, Australia*
[5]*School of Physics, University of Sydney NSW 2006, Australia*
[6]*ATNF, PO Box 76, Epping NSW 2121, Australia*

Accepted 1997 March 10. Received 1997 February 18

ABSTRACT

The radio sources in the galaxy cluster A3667 have been imaged using the Australia Telescope Compact Array at both 13 and 20 cm. The most striking source is a large region (at least 2.6 Mpc in extent) of mostly diffuse emission that is located to the north-west, well outside the central core of the cluster. Taking into account the X-ray and optical data, we suggest that turbulence in the outer region of the cluster, associated with a cluster merger, reaccelerates remnant relativistic particles, leading to the observed large region of radio emission. New MOST data which indicate similar diffuse emission to the south-east support this conclusion.

Key words: galaxies: clusters: individual: A3667 – radio continuum: galaxies.

1 INTRODUCTION

The cluster A3667 is an exceptional cluster of galaxies at a redshift of 0.055 (Sodré et al. 1992). There are several properties which distinguish it from the majority of clusters in the ACO catalogue (Abell, Corwin & Olowin 1989). It has a high velocity dispersion of about 1200 km s^{-1}, making it among the largest observed for any cluster (Sodré et al. 1992). It is also one of the brightest X-ray sources in the southern sky (Cooke et al. 1978; Edge, Steward & Fabian 1992), and the *Einstein* X-ray image shows extended emission with clear substructure (Sodré et al. 1992).

A3667 is associated with B2006 – 566, one of the largest and most complex of the strong radio sources in the southern sky. Radio imaging at arcmin resolution with the Molonglo Cross Radio Telescope at 408 MHz (Schilizzi & McAdam 1975), the Fleurs Synthesis Telescope (Goss et al. 1982) at 1415 MHz, and the Molonglo Observatory Synthesis Telescope (MOST) at 843 MHz (Jones & McAdam 1992) shows a giant diffuse source of low surface brightness with a steep spectral index, properties which classify it as a cluster halo or relic source.[1] Radio haloes are rare, with only 10 or so known (Hanisch 1982; Feretti & Giovannini 1995). Indeed, a recent search for radio haloes using a 38-MHz survey found no new examples (Lacy et al. 1993). This is surprising, since radio haloes have steep spectra and 38 MHz should be an optimum frequency for carrying out such a search. The clusters that contain haloes share similar characteristics. They all have high X-ray luminosities ($L \sim 10^{44}$–10^{45} erg s^{-1}) and large X-ray core radii (> 0.3 Mpc), and their galaxies have a high velocity dispersion. Recently, it has been found that their X-ray emission does not show the characteristics of a cooling flow (Burns et al. 1992; Edge et al. 1992; Jaffe 1992).

We observed A3667 at 13 and 20 cm using the Australia Telecope Compact Array (ATCA) to investigate further the connection between the X-ray and the radio structure. Here we present results from this investigation.

[1]In this paper we choose not to draw a distinction between halo and relic sources, but use the term 'halo' to refer generically to either class of diffuse cluster source.

2 OBSERVATIONS

2.1 ATCA observations

The ATCA observations were made simultaneously at 13 and 20 cm wavelengths, each with a total bandwidth of 128 MHz. We carried out a 4 × 12h synthesis, with complementary antenna configurations covering interferometer spacings from 30 m to 6 km. To image the northern part of the cluster which contains the halo source, we employed the mosaicking mode with 4 × 4 pointings. The 4-MHz spectral channels in each 128-MHz band were gridded separately to improve further the *uv* coverage on the longer baselines. For our final images we have adopted a resolution of 18 arcsec at both frequencies in order to preserve the extended

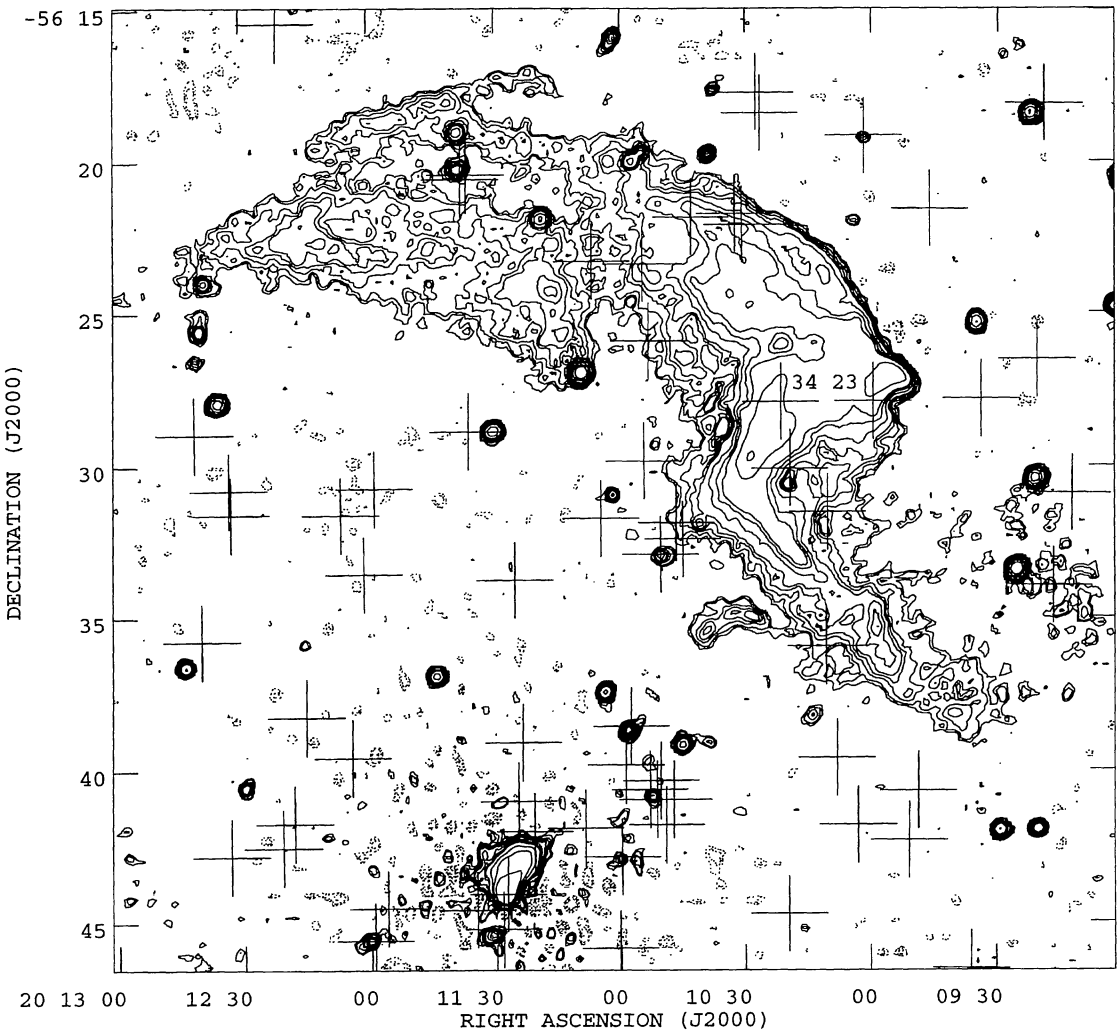

Figure 1. A contour representation of the central part of the 20-cm ATCA image covering the north-west region of A3667. The half-power beamwidth is 18 arcsec, and contours are at -0.8, -0.6, -0.4, -0.3, 0.3, 0.4, 0.6, 0.8, 1.0, 1.5, 2.0, 2.5, 5.0, 10 and 20 mJy beam^{-1}. The crosses indicate the location of galaxies from the sample of Sodré et al. (1992).

structure. The final, mosaicked images span 40×40 arcmin^2 with fairly uniform sensitivity (0.2 mJy beam^{-1} rms) and are sensitive to emission on scales up to $\sim$20 arcmin at 20 cm and $\sim$15 arcmin at 13 cm. The flux scale is based upon assumed flux densities for PKS B1934$-$638 of 16.2 Jy at 1380 MHz and 13.1 Jy at 2380 MHz.

In Fig. 1 we show a contour plot of part of the 20-cm mosaic. The crosses mark the positions of galaxies from the sample of Sodré et al. (1992), which contains 203 galaxies complete down to $b_{25}=18.0$, of which 128 have measured redshifts.

The most striking feature in the 20-cm image is the diffuse emission. Its total extent is 30 arcmin, which corresponds to 2.6 Mpc,[2] indicating that it is one of the largest radio sources known in the southern sky. From the 20-cm mosaic we measure a total flux density for the source of 2.6 Jy. The combined flux density of eight unresolved sources within the boundaries of the extended source is 150 mJy, giving a total flux density in extended emission of 2.4 ± 0.2 Jy. Because of our limited short-spacing data, this estimate should be regarded as a lower limit to the true flux density. The total flux density in the 21-cm Fleurs image is 1.5 ± 0.2 Jy (Goss et al. 1992), significantly lower than our ATCA estimate; we attribute this to the lower sensitivity of the Fleurs image (5 mJy beam^{-1} rms), leading to an area over which the source is detected that is a factor of 2–3 smaller. A similar procedure was applied to the low-resolution 13-cm image used to map the spectral index distribution (see below). The total flux density within the area of the extended emission is 1.5 Jy, and the contribution from the eight unresolved sources is 99 mJy, giving an extended flux density at 13 cm of 1.4 Jy.

Near the centre of the cluster (bottom centre of Fig. 1) is a strong discrete source B2007$-$569 (following the nomenclature of Goss et al. 1982). This is shown at higher resolution in Fig. 2, and confirms the suggestion of Goss et al. that the source is a head–tail (or, possibly, narrow-angle-tailed) radio galaxy. Galaxy number 072 in the list of Sodré et al. (1992) is only 2 arcsec from the radio peak, and is therefore

[2]We will use $H_0=50$ km s^{-1} Mpc^{-1} throughout.

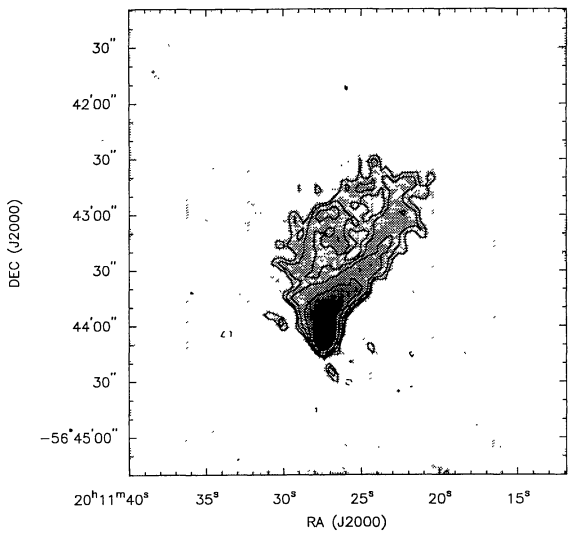

Figure 2. The 20-cm image of the central head-tail galaxy B2007 − 569 at a resolution of 5 arcsec. The contour levels are at − 2.5, − 1.5, − 1.0, 1.0, 1.5, 2.5, 5, 15, 25, 50, 150, 250 and 500 mJy beam^{-1}.

the likely optical counterpart. This is the same as galaxy 'd' identified by Goss et al.

2.2 Radio spectrum

The extended radio source has also been observed with MOST (Robertson 1991) at 843 MHz with a resolution of 43×43 cosec$|\delta|$ arcsec^2. A detailed discussion of these observations will be presented elsewhere. Following the same procedure used for the 13- and 20-cm ATCA images, we measure the total flux density of the extended halo at 843 MHz to be 5.5 ± 0.5 Jy; the error estimate includes the uncertainty in the determination of the zero-level in the image.

The MSH survey at 85.5 MHz gives the source flux density as 81 Jy (Mills et al. 1961), and the PKS survey at 408 MHz gives 12.2 Jy (Bolton, Gardner & Mackey 1964). Since we estimate the contribution of the eight point sources to be less than a few per cent, we take these two measurements as the flux density of the extended radio source.

The radio spectrum based on the MSH, PKS and MOST flux density measurements is consistent with a single power law with spectral index $\alpha = -1.1$ ($S_\nu \propto \nu^\alpha$). If we extrapolate this power law, then the ATCA data indicate either that the radio spectrum is steepening towards higher frequencies or that $\sim$20 per cent of the flux density is missed. Given the lack of short spacings in the ATCA observations, the latter is more likely.

Interpolating the low-frequency flux density measurements and assuming a redshift of 0.055, we find a monochromatic source power at 178 MHz of 4×10^{26} W Hz^{-1}.

2.3 Spectral index structure

In an attempt to locate the centre of activity in the halo source (and direct our search for optical counterparts) we formed a spectral index map from the images at 20 and 13 cm. To improve our sensitivity to the extended emission, we first convolved each image with a circular Gaussian of FWHM = 60 arcsec. The 20-cm image is slightly more sensitive to very smooth extended emission because of the smaller central gap in the *uv* plane. In calculating the spectral index we have included only pixels with intensities greater than 5.5 times the rms noise; the remaining pixels were blanked. The resulting spectral index map is shown in Fig. 3; as in Fig. 1, the crosses mark the galaxies from the Sodré et al. (1992) sample. Most of the point sources show an apparent gradient in spectral index, which may be due to the rather large convolved size on a slightly sloping background. However, the features in the spectral index distribution that are most relevant to our discussion occur on scales much smaller than those potentially affected by the lack of short spacings.

The head–tail source B2007 − 569 shows dramatic spectral steepening along the tail, from a fairly flat $\alpha = -0.4$ at the head down to $\alpha < -1.5$. This behaviour is common among head–tail galaxies (e.g. O'Dea & Owen 1986), and is attributed to ageing of the synchrotron electrons and a steepening of their energy distribution.

The spectral index structure of the extended region is interesting. It does not show a prominent gradient along the main axis of the whole source. Its most conspicuous feature is the region of fairly flat spectral index lying along the north-western rim, with marked steepening towards the south-east.

2.4 X-ray data

The *ROSAT* archive contained a PSPC image of A3667 in the energy range 0.1–2.4 keV with an integration time of 12 560 s. To enhance low surface brightness features, we have convolved the *ROSAT* image with a circular Gaussian of 60 arcsec FWHM. In Fig. 4 we show an overlay of part of this *ROSAT* X-ray image (contours) and the corresponding 20-cm ATCA image (grey-scale).

The X-ray isophotes in the central region are highly elongated, with clear evidence for substructure (see also Buote & Tsai 1996). We further note that the head–tail galaxy B2007 − 569 is associated with an X-ray point source, prompting a follow-up study of the association of head–tail galaxies with X-ray sources in clusters of galaxies (Edge & Röttgering 1995). In this paper, however, we will concentrate on the diffuse radio emission. The most striking aspect of the comparison of X-ray and radio images is that the extended radio source is clearly located beyond the detectable X-ray emission, although the sharp outer edges of the radio structure seem to follow the outer X-ray contours.

2.5 Galaxy distribution

In Fig. 5 we show the galaxy isodensity contours from Proust et al. (1988) for 423 galaxies brigher than $m_B = 19.0$, overlaid on a grey-scale of the 20-cm ATCA radio image. The galaxy distribution is bimodal, with the main concentration (A3667) centred on the brightest cluster galaxy, and a secondary concentration (S854 in the ACO catalogue) centred on the second-brightest galaxy. There is no radio emission associated with the main galaxy concentration, and the extended radio source is located north of the secondary concentration of galaxies.

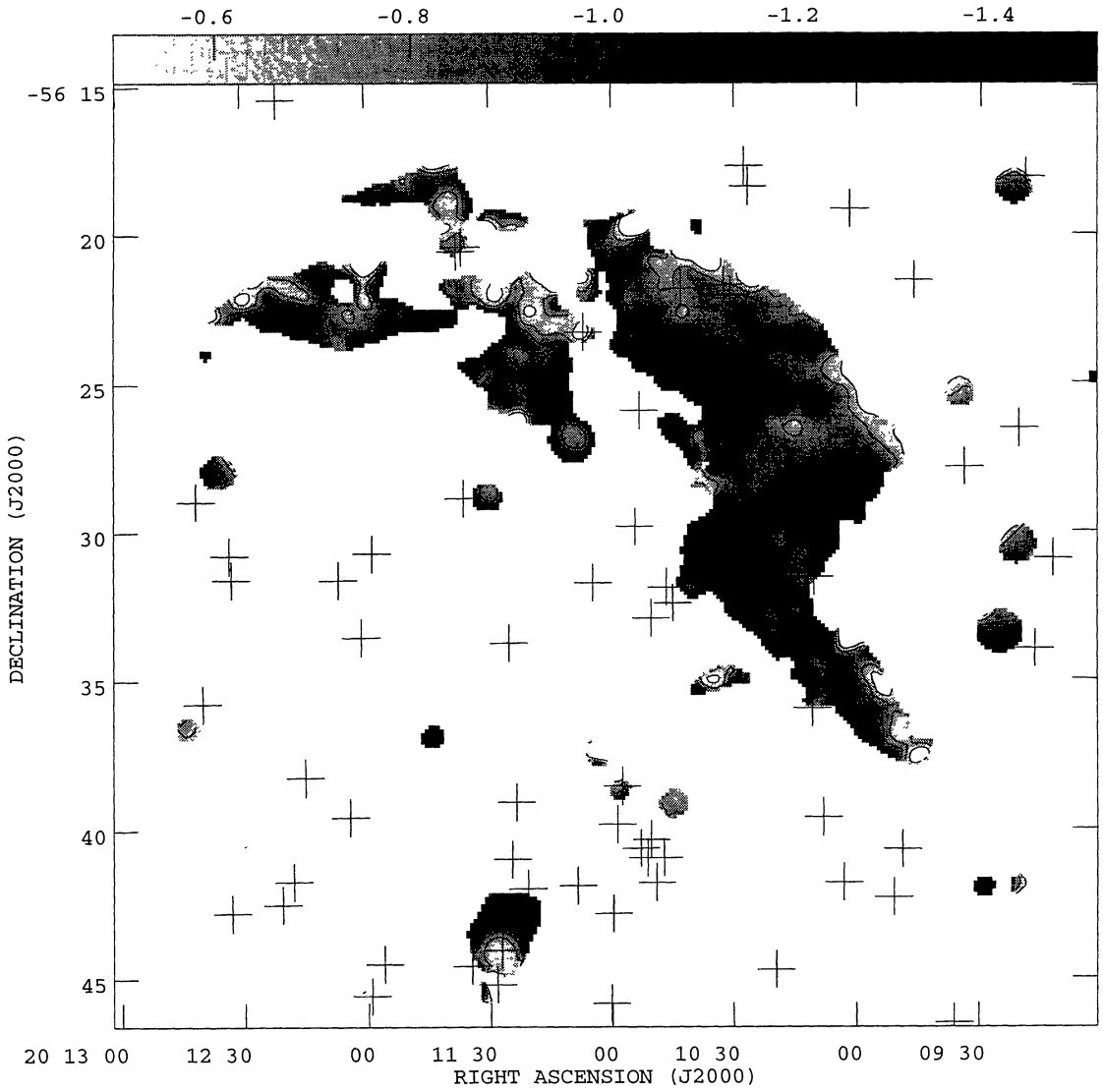

Figure 3. The spectral index distribution between 13 and 20 cm at a resolution of 60 arcsec. The contour levels correspond to spectral indices of $\alpha = -0.5$, -0.7, -0.9, -1.1, -1.3 and -1.5. The crosses mark the location of galaxies from the sample of Sodré et al. (1992).

2.6 Wide-field MOST data

Preliminary observations of an even larger field by MOST at 843 MHz reveal an additional weaker diffuse source to the south-east of A3667. The two diffuse sources can be seen straddling the X-ray distribution symmetrically in Fig. 6. The overall size including this south-east component is 1°, corresponding to 5.2 Mpc! More detailed ATCA observations of this region are proposed.

3 DISCUSSION

In interpreting the extended emission, we need to explain the main source of the relativistic electrons. Many models for smooth extended emission in radio clusters have been proposed (for reviews, see Jaffe 1992 and Feretti & Giovannini 1995). Such models explain the origin of the radiating electrons in the extended emission through (1) collisions with thermal protons in the cluster (Vestrand 1982), (2) generation in galactic wakes (Roland 1981), (3) turbulence and shocks in the intracluster medium (Harris, Kapahi & Ekers 1980; Tribble 1993), or (4) an active galactic nucleus (AGN).

In the case of the extended emission within A3667, none of the first three explanations seems tenable, mainly because the radio emission is located well outside the cluster centre. Explanation (1) operates in regions of high X-ray gas densities, i.e., not where the extended emission is located. Explanation (2) should work in areas of high galaxy density. Since the isodensity map of galaxies (Fig. 5) shows that the extended emission is not in a high-density region, explanation (2) seems to be ruled out. Both the X-ray and optical data strongly suggest that A3667 is undergoing a major merging event. Numerical hydrodynamical/*N*-body simulations of such events suggests that shocks will develop within the X-ray gas (Evrard 1990; Roettiger, Burns & Loken 1993; Burns et al. 1994a,b). Since the diffuse radio emission is outside the region where most of this shocked X-

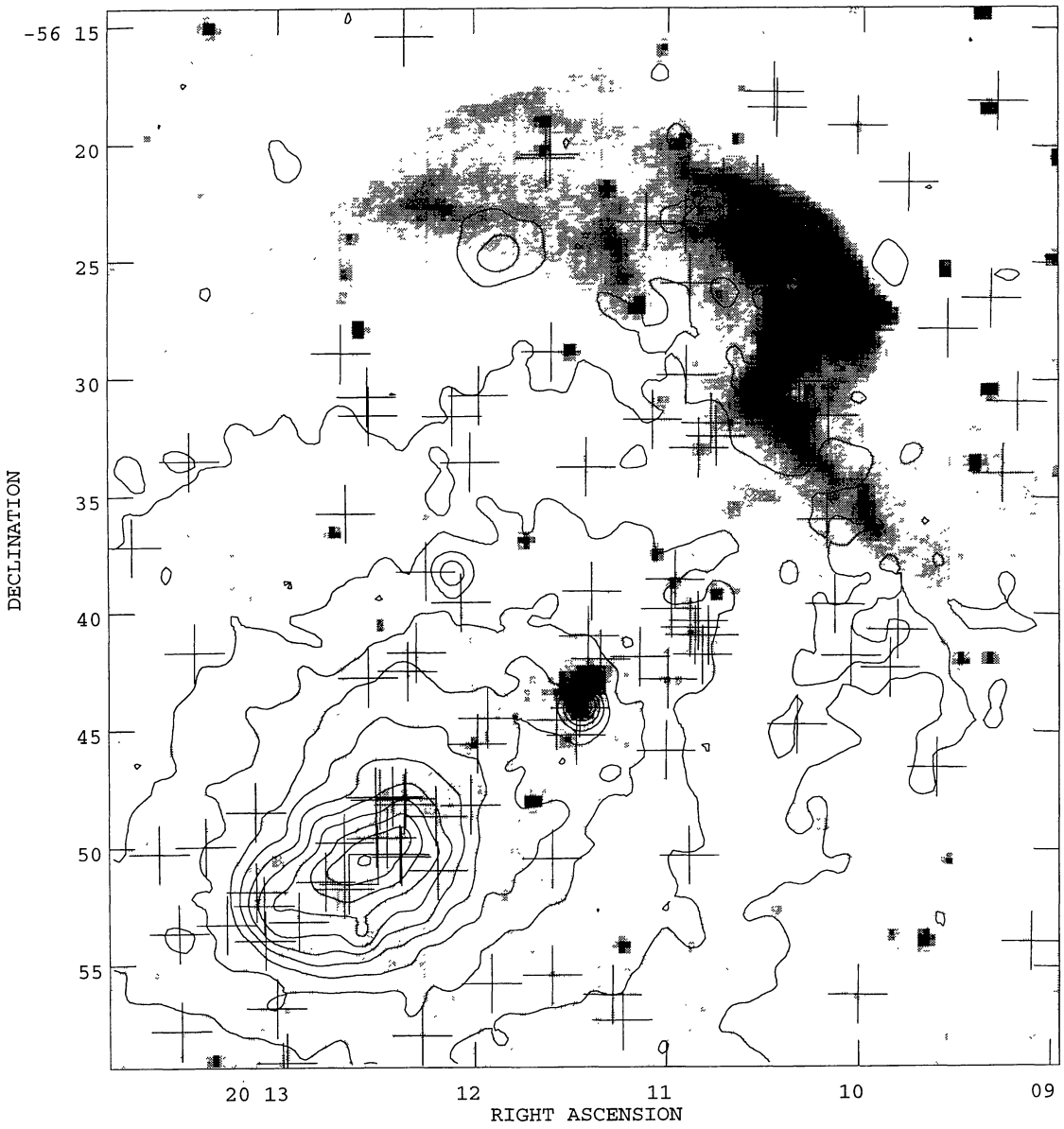

Figure 4. A contour representation of part of the *ROSAT* PSPC X-ray image in the energy range 0.1–2.4 keV, overlaid on a grey-scale of the 20-cm ATCA radio image. The contours are at 2, 8, 18, 32, 50, 72, 98, 128, 162, 200 and 242 times the background noise. The crosses represent galaxies for which the velocity data of Sodré et al. (1992) indicate cluster membership.

ray gas is supposedly located, explanation (3) is also not tenable.

A further possibility now suggested by the new MOST observations is that this is a giant (5.2-Mpc) radio galaxy centred on the cluster, with the diffuse emission interpreted as two edge-brightened radio haloes. This seems unlikely, because (i) it would be the second largest radio structure known (the largest radio source known is 3C 236 that has a linear size of 5.7 Mpc; Willis, Strom & Wilson 1974), (ii) other giant radio galaxies are not associated with rich clusters (but see Subrahmanyan, Saripalli & Hunstead 1996), and (iii) an obvious candidate for the central galaxy would be B2007 – 569, but this has a morphology very much like a head–tail source and not at all like the nucleus and inner jets of an FRII radio galaxy. On the other hand, the host galaxy of a putative giant radio galaxy could be another cluster member, possibly the cD, which is no longer active.

We now discuss the possibility that the source of relativistic electrons may be an AGN, either external to the diffuse source or embedded within it. First, we consider whether the head–tail galaxy B2007 – 569 could be the source of the electrons for the northern extended source. If this galaxy was falling towards the centre of the cluster and the radio tail was being stripped, possibly as a result of an encounter with gas asociated with the secondary cluster peak, this stripped tail might then provide the relativistic electrons in the halo region. A similar picture has been proposed for A2256 by Fabian & Daines (1991). However, such a scenario is probably not tenable, since one would

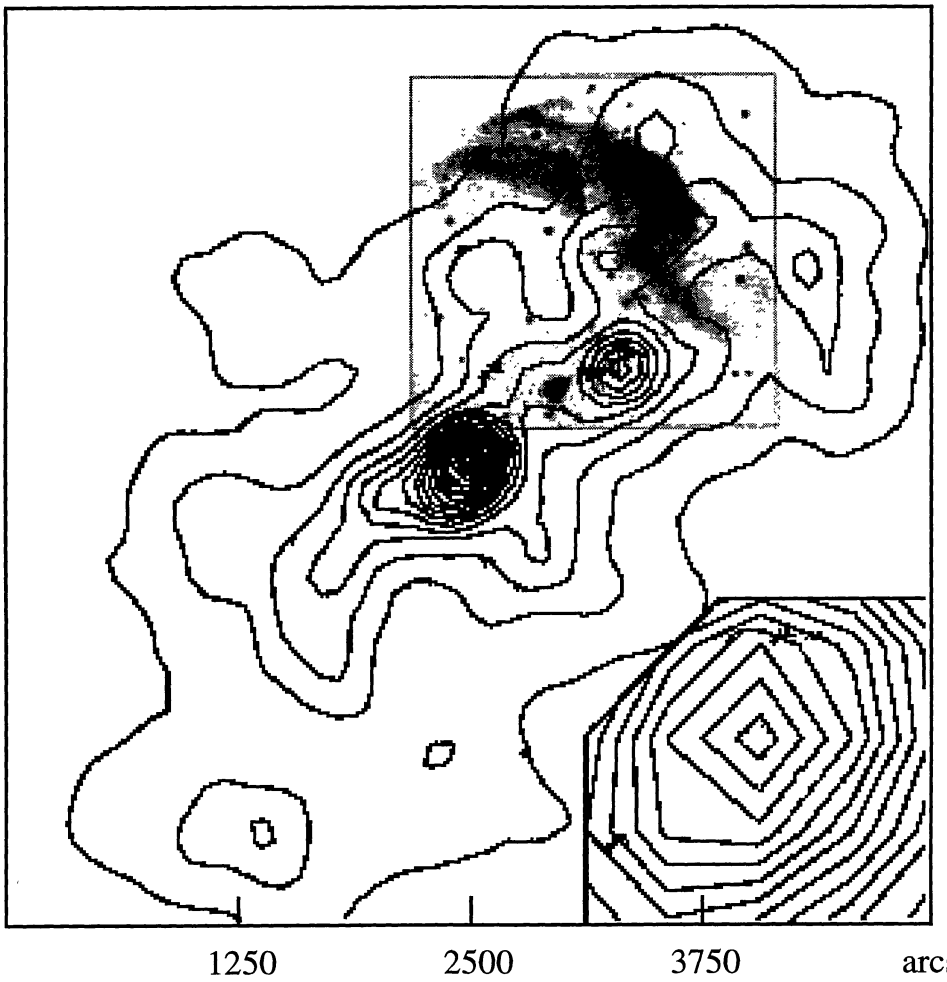

Figure 5. Galaxy isodensity contours for A3667 from Proust et al. (1988) for 423 galaxies brighter than $m_B = 19.0$. The background density is set to zero, and the density step is 58 galaxies deg^{-2}. An expanded plot of the cluster centre is shown on the lower right of the figure. The grey-scale is the 20-cm ATCA radio image (see also Fig. 1).

expect a faint bridge of emission connecting the head–tail galaxy to the diffuse extended emission (not seen in the ATCA 20-cm image). There is marginal evidence for such a bridge in the new MOST image (Fig. 6), but a better signal-to-noise ratio is required.

A second possibility is that the relativistic electrons originate in one or more AGN within the boundary of the extended emission itself. Unfortunately, the morphology and spectral index distribution do not suggest any obvious candidate galaxy. The two galaxies from the list of Sodré et al. (1992) that are located in regions of relatively bright radio emission are the galaxies 034 and 023 (see Fig. 1, where their locations are marked). However, neither galaxy can be associated plausibly with the radio structure. Furthermore, a deep AAT *R*-band CCD image obtained by one of us (RWH) suggests that both galaxies are spirals and therefore unlikely to harbor an AGN.

It is well known that if we invoke an AGN to provide the synchrotron-emitting electrons, it is difficult to explain the large size of halo sources without reacceleration of the electrons (e.g. Jaffe 1992, and references therein). The lifetime for electrons radiating at 1 GHz is about 10^8 yr. For electrons to diffuse over a region of ~ 1 Mpc, the implied velocities are 10^4 km s^{-1}. Since the Alfvén speed is probably not larger than 100 km s^{-1}, electrons can not travel through the halo while constantly radiating at 1 GHz (for a different view, see Holman, Ionson & Scott 1979).

The abrupt bending of some jets in wide-angle-tailed (WAT) radio sources is not well understood (e.g. Eilek et al. 1984; Norman, Burns & Sulkanen 1988). Recently, Burns et al. (1994a) argued that such bends are due to large-scale motions in the X-ray gas that accompany a cluster merger. Such motions could have velocities of ~ 800 km s^{-1} and persist in the cluster for 5 Gyr or so. Turbulence in the cluster medium associated with such motions might reaccelerate electrons as they traverse the cluster medium (see Tribble 1993, and references therein). In the case of A3667, this process would result in the regions with relatively flat spectral indices, and would produce the sharp boundaries in the radio emission. the turbulent effects of such a merger might be greater on the periphery of the cluster, outside the region dominated by the gas in the central deep potential well. This general explanation can be extended to explain the south-eastern component seen in the MOST observations.

Fitting a projected isothermal King profile to the X-ray

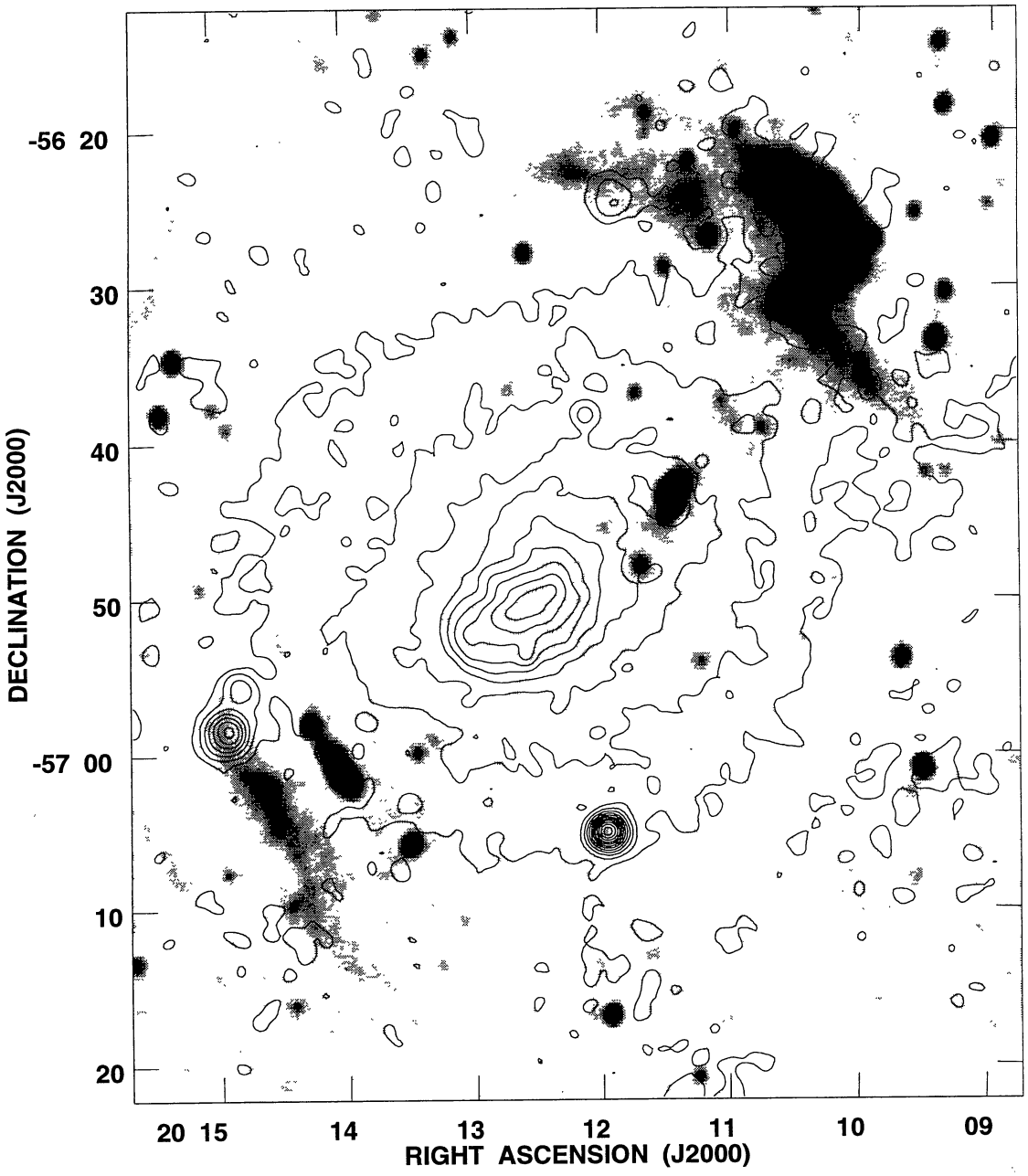

Figure 6. A contour representation of the *ROSAT* PSPC image (0.1–2.4 keV), overlaid on a grey-scale of the wide-field, 843-MHz MOST image. The rms noise level in the radio image is 0.7 mJy beam^{-1}. The X-ray contours are set at 2, 8, 18, 32, 50, 72, 98, 128, 162, 200 and 242 times the background noise.

isophotes yields estimates for the temperature and density of the X-ray gas in the region of the extended radio emission (e.g. Fabricant, Kent & Kurtz 1989). Using software kindly provided by Andy Fabian, we obtain a temperature of $\sim 10^8$ K and density of 10^{-4} cm^{-3}, resulting in a pressure of 1.4×10^{-12} dyne cm^{-2}. The equipartition pressure within the synchrotron plasma for flux densities in the range 0.5–5 mJy beam^{-1} yields pressures in the range of $(2–20) \times 10^{-14}$ dyne cm^{-2}, using standard assumptions (e.g. Röttgering et al. 1994). Although there are numerous ways to relax the assumptions so as to increase the equipartition pressure (e.g. Feretti et al. 1990), it seems plausible that the pressure in the X-ray gas is high enough to have a profound influence on the morphology of the radio source, for example, being capable of creating the sharp boundaries.

The bimodal galaxy distribution, the large velocity dispersion, the high X-ray luminosity and the distorted X-ray isophotes are all consistent with A3667 undergoing a massive merger. Another good example of an extended radio source in a merging cluster is A2256 (Briel et al. 1991; Röttgering et al. 1994). Such merging events seem capable of stopping a cooling flow (e.g. Fabian & Daines 1991), explaining why A3667 and A2256 do not have cooling flows. The turbulence in the cluster gas created during the merger

can reaccelerate electrons and heavily distort the morphology of cluster radio sources. Such a scenario is consistent with the suggestion of Burns et al. (1994a) that clusters containing WAT radio sources have undergone a relatively recent merger. We therefore consider the possibility that A3667 might have initially contained one or two WAT sources that provided the first synchrotron-emitting electrons in the diffuse regions. Subsequently, the WAT sources transformed into the halo source as a result of shocks and reacceleration of electrons. Therefore the radio source in A3667 might be in a relatively advanced stage in the merging process as compared with clusters containing 'normal' WAT radio sources. It has been claimed that the X-ray luminosity function shows dramatic evolution (e.g. Edge et al. 1990; Gioia et al. 1990), possibly indicating that clusters are relativey young objects, compared, for example, with galaxies. If the presence of halo sources is indeed linked to merging clusters, then the fact that they are rare in fainter samples of steep-spectrum radio sources (e.g. Lacy et al. 1993) might be attributed to the late formation of massive clusters. They will be rare also because both seed electrons and turbulence are necessary conditions.

ACKNOWLEDGMENTS

We thank Alastair Edge and Carolin Crawford for their help with the *ROSAT* data. We further acknowledge useful discussions with Andy Fabian, Richard Saunders and Peter Scheuer. HJAR acknowledges support from an EU twinning project and a programme subsidy granted by the Netherlands Organization for Scientific Research (NWO). The Australia Telescope is funded by the Commonwealth of Australia for operation as a National Facility managed by CSIRO. MOST is operated by the Unviversity of Sydney, partially supported by grants from the Australian Research Council. RWH acknowledges support for observatory travel from an ARC Institutional Grant.

REFERENCES

Abell G. O., Corwin H. G. J., Olowin R. P., 1989, ApJS, 70, 1
Bolton J. G., Gardner F. F., Mackey M. B., 1964, Aust. J. Phys., 17, 340
Briel U. et al., 1991, A&A, 246, L10
Buote D. A., Tsai J. C., 1996, ApJ, 458, 27
Burns J., Sulkanen M., Gisler G., Perley R., 1992, ApJ, 388, L49
Burns J., Rhee G., Owen F. N., Pickney J., 1994a, ApJ, 423, 94
Burns J., Roettiger K., Pinkney J., Loken C., Doe S., Owen F., Voges W., White R., 1994b, in Schlegel E., Petre R., eds, Proc. *ROSAT* Science Symp., AIP, New York, p. 183
Cooke B. A. et al., 1978, MNRAS, 182, 489
Edge A, C, Röttgering H. J. A., 1995, MNRAS, 277, 1580
Edge A., Steward G. C., Fabian A. C., Arnaud K. A., 1990, MNRAS, 245, 559
Edge A., Steward G. C., Fabian A. C., 1992, MNRAS, 258, 177
Eilek J. A., Burns J. O., O'Dea C., Owen F., 1984, ApJ, 278, 37
Evrard A., 1990, ApJ, 363, 349
Fabian A., Daines S., 1991, MNRAS, 252, 17P
Fabricant D., Kent S., Kurtz M., 1989, ApJ, 336, 77
Feretti L., Giovannini G., 1995, in Ekers R., Fanti C., Padrielli L., eds, Proc. IAU Symp. 175, Extragalactic Radio Sources. Kluwer, Dordrecht, p. 333
Feretti L., Spazzoli O., Gioia I., Giovannini G., Gregorini L., 1990, A&A, 233, 325
Gioia I. M., Henry J. P., Maccacaro T., Morris S. L., Stocke J. T., Wolter A., 1990, ApJ, 356, L35
Goss W. M., Ekers R., Skellern D. J., Smith R. M., 1982, MNRAS, 198, 259
Hanisch R. J., 1982, A&A, 116, 137
Harris D., Kapahi V., Ekers R., 1980, A&AS, 39, 215
Holman G., Ionson J., Scott J., 1979, ApJ, 228, 576
Jaffe W. J., 1992, in Fabian A. C., ed., Clusters and Superclusters of Galaxies. Kluwer, Dordrecht, p. 109
Jones P. A., McAdam W. B., 1992, ApJS, 80, 137
Lacy M., Hill G. J., Kaiser M. E., Rawlings S. G., 1993, MNRAS, 263, 707
Mills B. Y., Slee O. B., Hills E. R., 1961, Aust. J. Phys., 14, 497
Norman M. L., Burns J. O., Sulkanen M., 1988, Nat, 335, 146
O'Dea C., Owen F., 1986, ApJ, 301, 841
Proust D., Mazure A., Sodré L., Capelato H. V., Lund G., 1988, A&AS, 72, 415
Robertson J. G., 1991, Aust. J. Phys., 44, 729
Roettiger K., Burns J., Loken C., 1993, ApJ, 407, L53
Roland J., 1981, A&A, 93, 407
Röttgering H., Snellen I., Miley G., de Jong J., Hanisch B., Perley R., 1994, ApJ, 436, 654
Schilizzi R. T., McAdam W. B., 1975, Mem. R. Astron. Soc., 79, 1
Sodré L., Capelato H. V., Steiner J., Proust D., Mazure A., 1992, MNRAS, 259, 233
Subrahmanyan R., Saripalli L., Hunstead R. W., 1996, MNRAS, 279, 257
Tribble P. C., 1993, MNRAS, 263, 31
Vestrand W., 1982, AJ, 87, 1266
Willis A., Strom R. G., Wilson A. S., 1974, Nat, 250, 625